frontiers in Environmental Science

ORIGINAL RESEARCH
published: 08 July 2020
doi: 10.3389/fenvs.2020.00056

Functionalized Sawdust-Derived Cellulose Nanocrystalline Adsorbent for Efficient Removal of Vanadium From Aqueous Solution

Bongiwe Zulu[1], Opeyemi A. Oyewo[1], Bruce Sithole[2], Taile Y. Leswifi[3] and Maurice S. Onyango[1]**

[1] Department of Chemical, Metallurgical and Materials Engineering, Tshwane University of Technology, Pretoria, South Africa, [2] Council for Scientific and Industrial Research, University of KwaZulu-Natal, Durban, South Africa, [3] Department of Chemical and Civil Engineering, University of South Africa, Florida Campus, Pretoria, South Africa

OPEN ACCESS

Edited by:
Maria Graca Rasteiro, University of Coimbra, Portugal

Reviewed by:
Tiziana Tosco, Politecnico di Torino, Italy
Sajjad Khezrianjoo, Malayer University, Iran

***Correspondence:**
Opeyemi A. Oyewo
atiba.opeyemi@gmail.com
Maurice S. Onyango
Onyangoms@tut.ac.za

Specialty section:
This article was submitted to Water and Wastewater Management, a section of the journal Frontiers in Environmental Science

Received: *10 January 2020*
Accepted: *27 April 2020*
Published: *08 July 2020*

Citation:
Zulu B, Oyewo OA, Sithole B, Leswifi TY and Onyango MS (2020) Functionalized Sawdust-Derived Cellulose Nanocrystalline Adsorbent for Efficient Removal of Vanadium From Aqueous Solution. Front. Environ. Sci. 8:56. doi: 10.3389/fenvs.2020.00056

Water quality degradation due to noxious heavy metals has become a serious concern because of its impact on human health and the ecosystem. In this study, cellulose nanocrystal (CNC) derived from sawdust as a green renewable and sustainable resource was functionalized and used as adsorption media to remove pentavalent vanadium (V) from aqueous solution. The physicochemical properties of the adsorbent were studied using various characterization techniques such as Fourier transform infrared (FTIR) spectroscopy, scanning electron microscopy (SEM), and X-ray diffraction (XRD). The performance of the functionalized CNC adsorbent was explored as a function of solution pH, temperature, adsorbent mass, time, and initial concentration in batch adsorption. XRD results confirmed the crystalline nature of the CNC, which was more pronounced upon modification. The SEM micrograph revealed rough surface and high porosity, which suggested that the CNC possessed prerequisite properties of a good adsorbent. From the FTIR spectra results, the interaction between anionic vanadium species and functionalized CNC was confirmed by the reduction in wavelength of carboxylic groups (–COOH) of the CNC. Meanwhile, from the adsorption results, V removal efficiency was found to be affected by solution pH, temperature, adsorbent mass, and initial concentration. The Langmuir maximum adsorption capacity was 37.9–47.2 mg/g in the temperature range studied. In evaluating the reusability of the CNC through adsorption–desorption studies, results confirmed that the functionalized CNC could be used more than once with about 20% reduction in adsorption of V in each adsorption–desorption cycle. So far, there are indications that modified CNC may be an alternative adsorption media for V.

Keywords: adsorption, cellulose nanocrystals, functionalization, sawdust, vanadium

INTRODUCTION

Mining and metallurgical industries are the largest contributors to South Africa's economy but are at the same time the major contributors to water pollution crisis (Roy et al., 2019). These industries release large quantities of untreated (waste) water containing high level of heavy metal pollutants. In particular, toxic metals such as mercury, chromium, copper, zinc, lead, and vanadium have been found in waste streams (Parmar and Thakur, 2013). Among these metals, vanadium has been recognized as one of the most dangerous pollutants in the same class with mercury, lead, and arsenic (Hegazi, 2013). Prolonged exposure to high levels of vanadium is known to cause damage to the human respiratory organ and can also increase the risk of cancer related to lungs (Li et al., 2019). Vanadium is not biodegradable (Carolin et al., 2017); therefore, contaminated effluents need to be treated using robust techniques that ensure either its complete removal or reduction to acceptable levels that comply with environmental regulatory laws.

Various treatment techniques have been explored in vanadium (V) removal from contaminated effluents. These include chemical precipitation, ion exchange, chemical oxidation, reverse osmosis, ultrafiltration, electrodialysis, and adsorption (Montaña et al., 2013; Mulas et al., 2017). These techniques have inherent negative features such as high operation cost, the requirement of highly skilled personnel to operate, slow kinetics, incomplete removal of the metal ions and creation of hazardous metal-containing sludge which are difficult to treat (Quesada et al., 2019). These challenges hinder their wide application, especially in less developed countries. Proponents of adsorption technology in water treatment argue that the technology is robust, low cost if appropriate adsorbents are used, and associated with low environmental footprint when the adsorbents are reused multiple times before disposal. Consequently, several studies have reported the use of adsorption technology in V removal (Burakov et al., 2018). In the algorithm of adsorption process development, one of the starting points is the selection of an appropriate adsorbent. In this regard, a good adsorbent should have several features such as high affinity for the target pollutant, availability (abundance), fast kinetics, high selectivity, low cost per unit of polluted water treated, and renewable (Al-ghouti and Da'ana, 2020). In respect to these properties, various researchers have studied the performance of activated carbons, zeolites, clays silica gel, metal oxides, and biosorbent in vanadium removal (Barakat, 2011; Ince and Ince, 2017). Most of these materials do not provide high capacity for vanadium uptake and therefore would require large fixed beds.

The forestry, timber, pulp, and paper (FTPP) industries produce a lot of cellulosic waste materials that pose disposal problems. The use of these wastes as adsorbents can significantly contribute to environmental protection and reduce the cost of water treatment (Putro et al., 2017). Recently, nanoscale solid materials derived from these wastes have dramatically received tremendous attention because of their attractive advantages including eco-friendliness, cost-effectiveness, high efficiency, reusability, and possibility of metal recovery (Mahfoudhi and Boufi, 2017). Out of the variants of nanoscale cellulosic materials, cellulose nanocrystals (CNC) have large specific surface area with hydroxyl and anionic sulfate ester groups, which make the CNC a perfect substrate for preparing composites for adsorption of heavy metals from water and wastewater (Abdullah et al., 2013; Kumar et al., 2017).

Vanadium exists in an aqueous environment as an oxyanion, which is negatively charged. The charge on the CNC structure is also negative (Jiang et al., 2020). Consequently, CNC in its pristine form cannot be efficient for vanadium removal. The CNC matrix must, therefore, be re-engineered to make it suitable for adsorption of vanadium. Cationic surfactants are considered to be the most prominent materials for the enhancement of the adsorption capacity of adsorbents via functionalization (Hokkanen et al., 2016). So far, hexadecyltrimethylammonium bromide (HDTMA-Br) has been the most utilized surfactant for surface modification of CNC due to its ability to enhance the surface affinity of the CNC (Kaboorani and Riedl, 2015; Lizundia et al., 2016). To date, there is limited information available on the application of functionalized CNC derived from sawdust as an adsorbent for the removal of vanadium ions from water. Therefore, it is worthwhile to design a simple modification route to synthesize functionalized CNC adsorbent with tailored properties, while preserving their original morphology and maintaining the integrity and strength of the crystal.

This study presents the development of a simple route for cationic surfactant functionalization of CNC as an adsorbent for remediation of V pollutant from water. Upon functionalization, the adsorption media was characterized to obtain important features of the adsorption media and insights into V adsorption mechanism. Thereafter, batch adsorption studies were conducted to determine the adsorption capacity and kinetics characteristics of V. The effects of solution pH, sorbent mass, contact time, initial ion concentration, and temperature were systematically investigated. The equilibrium and kinetics data were interpreted using appropriate models.

MATERIALS AND METHODS

CNC suspension derived from sawdust was supplied by CSIR-Durban (South Africa) and was used as raw material for the preparation of sorption media. HDTMA-Br, ammonium metavanadate (NH_4VO_3), sodium hydroxide pellets (NaOH), and hydrochloric acid (HCl, 32% concentration) were purchased from Sigma-Aldrich (Germany). De-ionized water produced with the Purite water system (Model Select Analyst HP40, UK) was used to prepare relevant solution concentrations throughout this study. All chemicals used were of analytical grade.

Functionalization of CNC Adsorbent

The procedure for CNC involved a one-pot synthesis route using deionized (DI) water and sulfuric acid, which were subsequently ultra-sonicated to afford CNC suspension (Gibril et al., 2018; Sithole, 2019). The HDTMA-Br solution was prepared separately by mixing 0.73 g of HDTMA-Br powder with 48 ml of DI water and heated at 45°C under magnetic stirring. The modification reaction was initiated by introducing 35.09 g of 2.0% consistency CNC suspension into a 300-ml triple neck round bottom flask.

Trials confirmed that about 17 ml of the prepared HDTMA-Br solution was suitable for the modification of the amount of CNC used in synthesis procedure and was added slowly under continuous stirring for 2 h. Thereafter, the suspension was washed with DI water and then centrifuged for 45 min at 40,000 rpm to remove any possible excess of quaternary ammonium salt that could have aggregated on the CNC surface. The functionalized CNC sample was then removed from the centrifuge, filtered, and air-dried for 5 days at room temperature. Finally, the obtained dry cake was crushed into a fine powder and is hereafter referred to as HDTMA-Br functionalized CNC (HDTMA-Br/CNC) adsorbent.

Preparation of Vanadium Synthetic Water

A 1,000 mg/L stock solution of V was prepared by dissolving 2.2960 g of NH_4VO_3 powder in DI water using a 1-L volumetric flask while heating at ∼200°C. The working solution concentrations for batch equilibrium and kinetic experiments were obtained by diluting stock solution to appropriate concentrations.

Characterization of Adsorbent

Fourier transform infrared (FTIR) spectroscopy, X-ray diffraction (XRD), and scanning electron microscopy (SEM) were used to study different physical and chemical features of the HDTMA-Br/CNC adsorbent. The FTIR spectrometer (Perkin–Elmer Spectrum 100 spectrometer) equipped with an FTIR microscopy accessory, on the attenuated total reflection (ATR) diamond crystal was used to determine the functional groups present on the surface of the adsorbent. All spectra were recorded in the frequency range of 500–4,000 cm^{-1} with a spectra resolution of 4 cm^{-1}. To ascertain surface morphology of functionalized CNC adsorbent before and after adsorption process, SEM analysis was performed using a JEOL JSM-7500F FE-SEM equipped with an SEM-EDS analyzer running at a 2-kV accelerating voltage. The X-ray powder diffraction pattern was obtained using a Panalytical X'Pert Pro MPD-Ray diffractometer equipped with an X'celerator detector and operated with Ni-filtered Cu Kα radiation ($\lambda = 0.15406$ nm) generated at a voltage of 45 kV and a current of 40 mA.

Batch Adsorption Studies

Batch adsorption equilibrium experiments were carried out to determine the efficiency of the developed adsorbent on V removal as a function of variables such as adsorbent mass, initial solution pH, and temperature. Known amounts of the adsorbent were placed in contact with V solutions of known initial concentrations in 100 ml of polyethene (PE) plastic sample bottles. The contact between V solution and the adsorbent was facilitated by agitation in a temperature-controlled thermostatic shaker operated at 160 rpm for 24 h. The solution pH was varied from pH 2 to 8, temperature from 298 to 318 K, and adsorbent mass from 0.025 g to 0.2 g. At the end of each experiment, the samples were centrifuged for 45 min at 40,000 rpm and then filtered using a 0.45-μm syringe filter and were analyzed for residual metal ion concentration using an inductively coupled plasma atomic emission spectrometer (ICP-AES, 9000, Shimadzu, Japan). To determine the adsorption efficiency and uptake of V onto HDTMA-Br/CNC adsorbent, Equations 1 and 2 were used, respectively:

$$R_t = \frac{C_o - C_e}{C_o}.100 \quad (1)$$

$$q_e = \frac{C_o - C_e}{m}.V \quad (2)$$

where q_e is the adsorption capacity (mg/g) C_o and C_e are the initial and equilibrium concentrations (mg/L) of polluting ion, respectively. V is the volume (L) of the solution and (m) is the weight (g) of the adsorbent.

The kinetic experiments were conducted using a 1-L batch reactor stirred at a speed of 220 rpm. The effect of initial concentration was explored by varying the V initial concentration from 25 to 75 mg/L. The pH and adsorbent mass were fixed in the kinetic experiments. At various time intervals, a known amount of sample was taken and immediately filtered using a syringe filter of 0.45 μm pore size. Thereafter, the filtered samples were analyzed for residual V using an inductively coupled plasma atomic emission spectrometer (ICP-AES, 9000, Shimadzu, Japan). The amount of V adsorbed onto modified-CNC at the time (t) was evaluated using Equation 3:

$$q_t = \frac{C_o - C_t}{m}.V \quad (3)$$

where q_t is the time-dependent amount of V adsorbed per unit mass of adsorbent and C_t is the concentration of V at any time t.

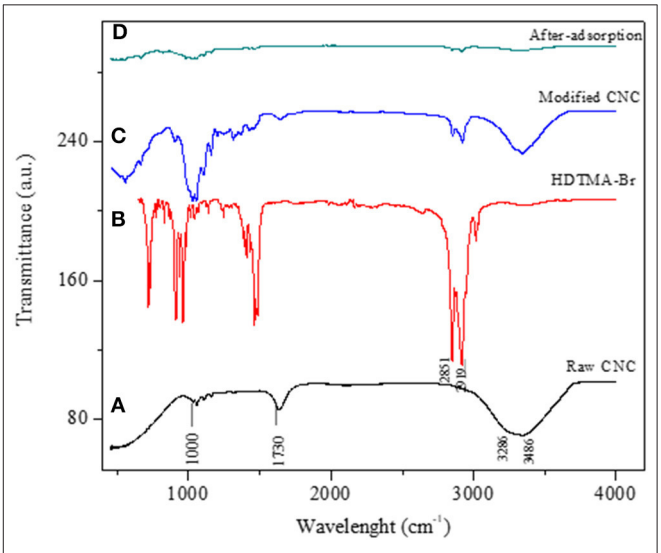

FIGURE 1 | FTIR spectra of **(A)** raw CNC (unmodified), **(B)** HDTMA-Br, **(C)** HDTMA-Br/modified CNC, and **(D)** HDTMA-Br/modified CNC after-V adsorption.

All the adsorption experiments were conducted in duplicate and the average values are reported.

Adsorption–Desorption Studies

The reusability of the adsorbent is an important factor in determining the economic viability of an adsorption process. In this regard, the adsorption–desorption study was conducted to assess the number of cycles the HDTMA-Br/CNC adsorbent would be used before replacement. The adsorption part of the cycle was done as described in adsorption experimental section while desorption of V from the surface of spent adsorbent was investigated using deionized water, NaCl and HCl eluents. As such, the spent adsorbent was dried and dispersed in the different eluents and then the mixtures were placed in a thermostatic bath shaker operated at 160 rpm and 298 K for 24 h. Thereafter, the desorbed solution was analyzed using ICP-AES to determine the amount of V desorbed. The adsorption–desorption procedure was repeated three times, and for each cycle, the percentage desorption efficiency was determined using the following equation:

$$\%\ Desorption\ efficiency = \frac{released\ Vconcentration}{initial\ adsorbed\ V} \quad (4)$$

RESULTS AND DISCUSSION

FTIR Spectroscopy

FTIR spectroscopy is an important tool for studying the functional groups incorporated onto the surface of an adsorbent and also to confirm the changes after surface modification. The FTIR spectra of raw CNC (unmodified), pure HDTMA-Br, and HDTMA-Br-modified CNC and the material after adsorption of V are shown in **Figures 1a–d**, respectively. The bands around 2,919 and 2,851 cm^{-1} in both pure HDTMA-Br and modified CNC are due to the characteristic symmetric and

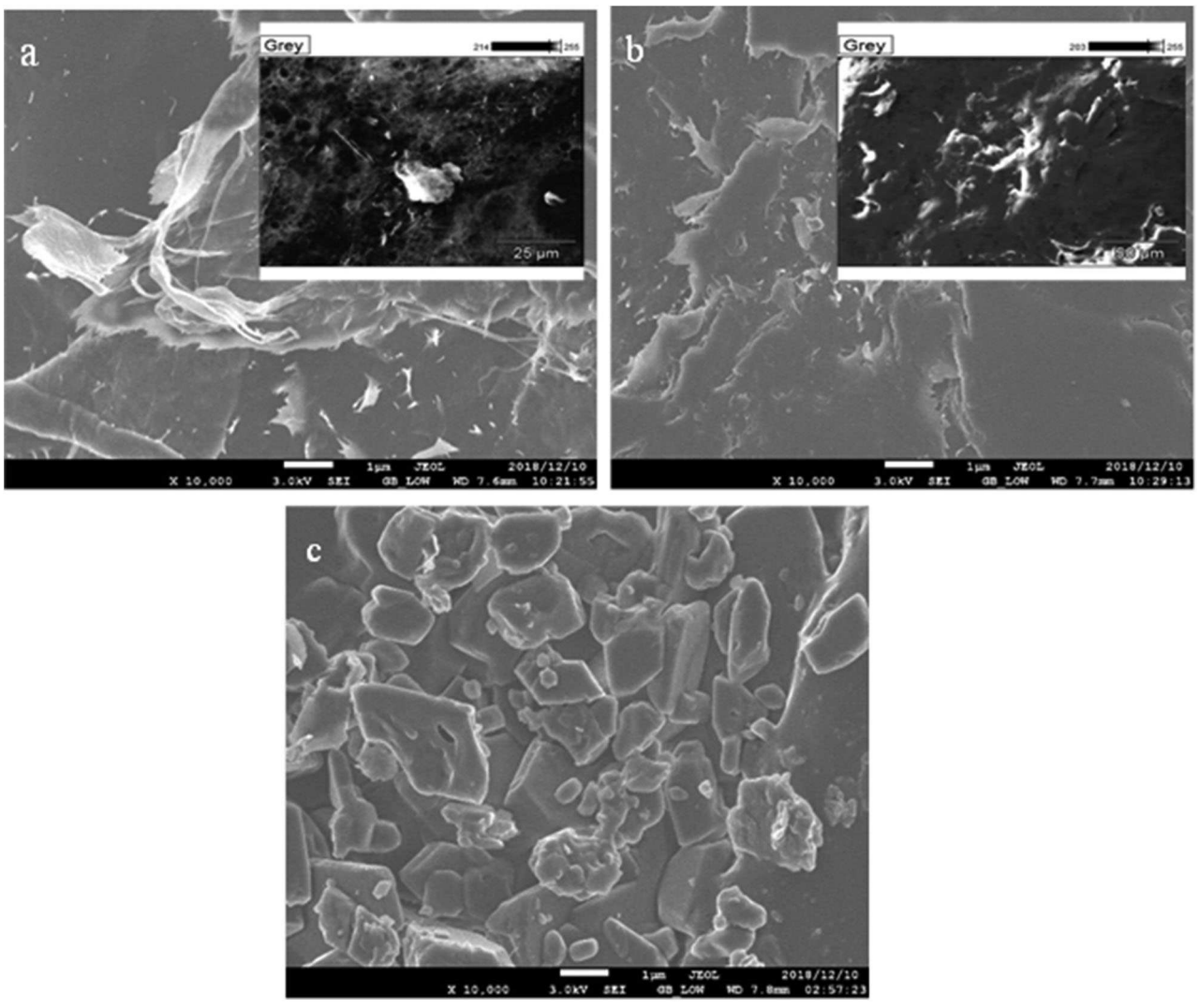

FIGURE 2 | SEM images of **(a)** raw CNC (unmodified) and **(b)** HDTMA-Br/modified CNC **(c)** HDTMA-Br/modified CNC after-V adsorption.

asymmetric C–H stretching vibrations of methyl and methylene groups (Kaboorani and Riedl, 2015). In the spectrum of raw CNC, the peak at 3,850 cm^{-1} could be ascribed to the O–H stretching vibrations on the surface of CNC. The peak at 1,730 cm^{-1} is the CO of a carbonyl group and could be attributed to the presence of carboxylic groups responsible for the coordination of metal ions during the adsorption process due to its disappearance in the spectrum of spent adsorbent (**Figure 1a**). The vibrational frequency at 1,250 cm^{-1} is due to the asymmetrical S=O vibration, which confirms the presence of a sulfate group present on the surface of pristine CNC. This functional group was formed during acid hydrolysis of CNC by sulfuric acid (Singh et al., 2015). A reduction in the intensity of the O–H band is noticeable upon functionalization (**Figure 1c**), and this phenomenon could be due to a reduction in the degree of the hydrogen bonding associated with –OH vibrations (Bezerra et al., 2017). A shift in the position of certain peaks after the adsorption of V is also observed, and this could be attributed to the interaction of the CNC with vanadium during the adsorption process.

Scanning Electron Microscopy

SEM analysis was used to explore the surface or external morphology of CNC adsorbent. **Figure 2** shows the SEM images of (a) raw CNC, (b) HDTMA-Br-modified CNC, and (c) HDTMA-Br/CNC after vanadium adsorption, respectively. **Figure 2a** shows that the raw CNC possessed a high porous surface and also indicates that CNC has high cellulose content with the average particle size between 6 and 36 nm (Nkalane et al., 2019). **Figure 2c** demonstrates a noticeable coverage of pores by the adsorbed vanadium ions after the adsorption process. Also, EDS analysis (**Table 1**) reveals a high percentage of carbon, oxygen and other elements corresponding to their binding energies as expected in all nanocellulose materials. As such the pristine CNC possesses mostly carbon (62.91%) and oxygen (33.15%). However, the presence of vanadium confirms the adsorption of V on the surface of modified CNC due to chemical interaction between V ion and modified CNC during the adsorption process.

X-Ray Diffraction

The crystallinity analysis of CNC adsorbents (unmodified, modified, and spent modified CNC) is presented in **Figure 3**. The XRD patterns in these cellulose samples show two major peaks at 15.51° and 22.4° corresponding to the 101 and 002 crystalline planes, respectively, ($C_{60}H_{88}O_8$ and $C_2H_{192}N_{64}O_{16}$), which are assigned to the cellulose 1α and 1β phases (Schwanningerab, 2004). However, this intensity is more pronounced upon modification and after adsorption of V, suggesting an increase in very strong interactions between the HDTMA-Br and cellulose structure. The appearance of other additional phases at 30° is also noticed after modification of CNC, which is further ascribed to the presence of modifiers used in the synthesis of modified CNC (Yin et al., 2018). Overall, the phases identified on CNC used in this study are similar to the reported characteristics of pure cellulose reported in our previous studies (Nkalane et al., 2019).

TABLE 1 | EDS analysis of raw CNC modified CNC before and after adsorption.

Element wt.%	Raw CNC	Modified CNC	After V adsorption
C	62.91	57.88	76.92
O	33.15	37.51	14.27
Na	0.25	-	-
Mg	0.04	0.03	-
Al	0.09	1.72	0.75
Si	0.06	0.03	0.05
S	3.30	1.28	-
Ti	-	0.18	-
Cl	0.11	-	-
V	-	-	7.92
Cu	-	-	0.09
K	0.03	-	-
Ca	0.04	-	-
Br	-	1.37	-
Cr	0.03	-	-
Total	100	100	100

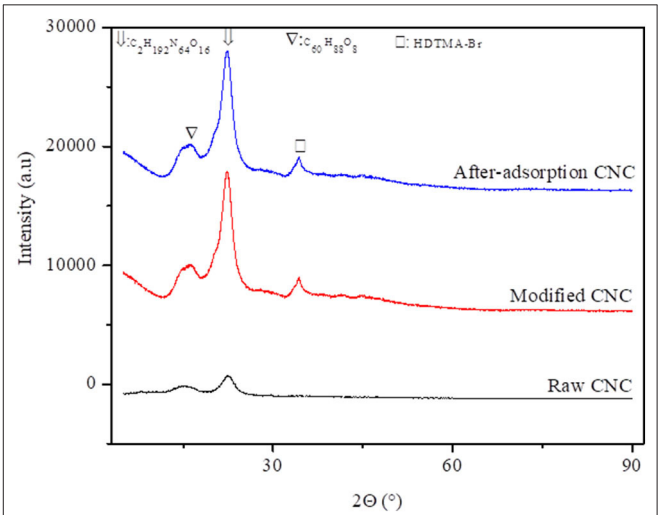

FIGURE 3 | X-ray diffraction patterns of unmodified, modified, and after V adsorption formed of cellulose nanocrystals.

Effect of Initial Solution pH

The pH of the metal ion solution is a very important variable that affects the degree of ionization and hence the adsorption process (Salehi and Anbia, 2019). Therefore, the effect of the initial solution pH on V uptake onto the surface of the surfactant-modified CNC was investigated in the pH 2–8 range. The results, summarized in **Figure 4**, show that highest V uptake is achieved at pH 3.0–4.0. This is because of the change in the chemistry of vanadium ion in aqueous solution with a change in pH. Vanadium has been reported to oxidize to its pentavalent anion (VO_3^-) at $3 < pH > 5$ in aqueous solution. This narrow pH range is the most conductive region for the adsorption of V ion

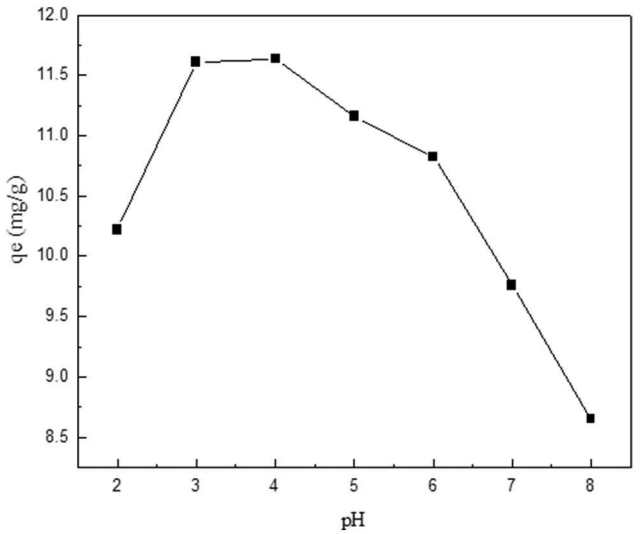

FIGURE 4 | Effect of initial pH on V adsorption onto modified CNC adsorbent (initial concentration, 25 mg/L; temperature, 298 K; adsorbent dose, 0.1 g).

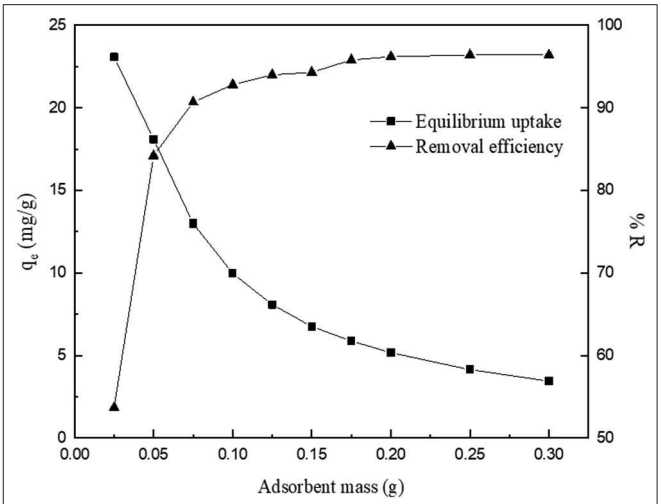

FIGURE 5 | Effect of adsorbent dosage on the removal of V onto modified CNC (initial concentration, 25 mg/L; pH 4.01; temperature, 298 K).

on the positively charged adsorbent surface. Meanwhile, below or above the optimum pH range, lower adsorption values are observed. In a study by Mthombeni et al. (2016) to investigate the effect of solution pH on the adsorption of V, a similar trend was observed, which can be ascribed to the decrease in the removal efficiency at pH 3.0 to the existence of VO_2^+ ions, which promoted the electrostatic repulsion of the protonated amino groups of the adsorbent. Besides, the decrease in adsorption uptake at increased initial pH might be attributed to the increased OH^- concentration on the surface of the adsorbent at high solution pH, which enhanced competitive adsorption with vanadium oxyanions.

Effect of Adsorbent Mass

The effect of modified CNC mass on the V uptake efficiency shows that the percentage of V removed increased with an increase in the adsorbent dosage (**Figure 5**). This is because at high adsorbent mass, the active sites for V uptake form solution increases (Mojiri et al., 2017). However, metal ion uptake decreases from 23.08 to 3.46 mg/g, with an increase in the dose from 0.025 to 0.3 g. Similar results were reported on the adsorption of V using adsorbent derived from agricultural waste (Kajjumba et al., 2018). Also, the results reveal that at higher sorbent dosage beyond 0.1 g, a slight increase in adsorption efficiency was attained. This is attributed to possible aggregation of particles of the adsorbent at higher dose, causing overlap and overcrowding during the process, and hence resulting in a decrease in accessibility of the available adsorption sites. Hence, in this study, 0.1 g was used for subsequent experiments.

Adsorption Isotherms

The temperature dependence of V adsorption onto modified CNC from simulated water was explored by varying the temperature from 298 to 318 K. The relationship between the amounts of adsorbed ions per unit mass of the CNC adsorbent (q_e) and the equilibrium concentration (C_e) of V solution is shown in **Figure 6A**. It is observed that the adsorption capacity of V increased with an increase in metal ion concentration and temperature of the system, suggesting that the adsorption of V onto modified CNC is endothermic in nature. The enhanced adsorption at higher temperature might be due to the increase in the diffusion rate of metal ions across the external boundary layer and into the internal pores of the adsorbent particles (Ahmad et al., 2015). The data obtained from adsorption equilibrium are used to describe the interaction between adsorbate and adsorbent for effective design of an adsorption process. Subsequently, the experimental data were analyzed using Langmuir, Freundlich, and Temkin models (**Table 2**). The linear form of the Langmuir, Freundlich, and Temkin adsorption isotherm equations (Onyango et al., 2004; Mthombeni et al., 2016) are given in Equations 5–7, respectively:

$$\frac{C_e}{q_e} = \frac{C_e}{q_m} + \frac{1}{k_L q_m} \tag{5}$$

$$\ln q_e = \ln k_f + \frac{1}{n} \ln C_e \tag{6}$$

$$q_e = \frac{RT}{b} \ln A + \frac{RT}{b} \ln C_e \tag{7}$$

where C_e is the equilibrium concentration of the polluting ion (mg/L), q_e is the amount of vanadium ions adsorbed on the adsorbent at the equilibrium (mg/g), q_m is the maximum adsorption capacity that describes a complete monolayer adsorption (mg/g), k_L is the Langmuir isotherm constant (L/mg) related to the free energy of adsorption, k_f and N are the Freundlich constants, R is a gas constant 8,314 J/mol·K, and T is the adsorption process temperature in K; A_T is the Temkin isotherm equilibrium

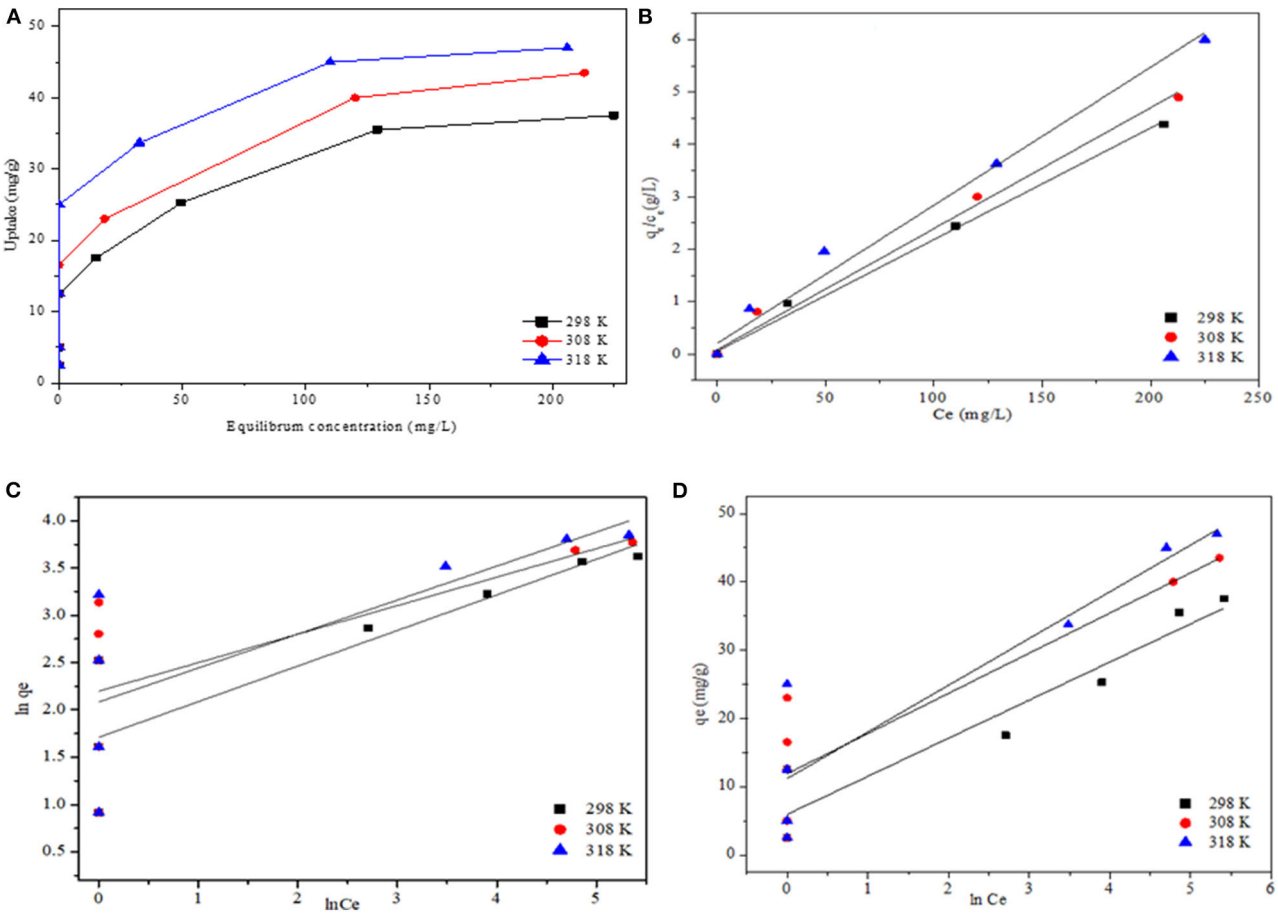

FIGURE 6 | Effect of temperature on V adsorption onto modified CNC **(A)**. Adsorption isotherm **(B)** and equilibrium data fit to Langmuir isotherm model, **(C)** Freundlich isotherm model, and **(D)** Temkin isotherm model.

TABLE 2 | Summary of equilibrium isotherms parameters of V sorption onto modified CNC.

Temperature °K	Langmuir			Freundlich			Temkin			
	q_m (mg g^{-1})	B (L mg^{-1})	R_L	R^2	K_F (L g^{-1})	n	R^2	b_T	A_T	R^2
298	37.9	0.13	0.221	0.987	5.536	2.66	0.786	417.73	2.48	0.929
308	43.3	0.28	0.939	0.994	9.017	3.32	0.501	215.20	2.54	0.820
318	47.2	0.41	0.704	0.996	8.039	2.78	0.601	236.35	2.27	0.846

binding constant (L/g) and b_T is constant related to heat of sorption.

The equilibrium isotherm parameters were extracted from the linear plots presented in **Figures 6B–D** and are summarized in **Table 2**. Based on the correlation coefficients, only the Langmuir isotherm describes the adsorption process sufficiently well. This may be an indication of adsorption on homogeneous surfaces. The results further show an increase in the Langmuir maximum adsorption capacity (q_m) and $k_L$from 37.9 to 47.2 mg/g and 0.130 to 0.410 (L/mg), respectively, with an increase in temperature. Compared with other biomaterials summarized in **Table 2**, the adsorption capacity obtained in this study is quite competitive. In exploring the favorability of the adsorption process using the separation factor (R_L), results reveal that the values are within $0 < R_L > 1$ range, indicating that the adsorption of V onto modified CNC was favorable. Overall, the adsorption capacity obtained in this study is highly competitive compared to the performances of some adsorbents reported in the literature with the same operating condition (see **Table 3**).

Adsorption Kinetics

Adsorption kinetics is useful in determining the rate of adsorption and the mechanism involved in the removal of any

contaminant from water. In the present study, the effect of the initial concentration in the range 25–75 mg/L was investigated as a function of contact time (0–280 min), and the results are summarized in **Figure 7**. The graph presents a two-step process: an initial stage characterized by rapid adsorption as a result of the availability of sufficient binding sites and a second stage in which the rate gradually decreases as equilibrium stage is approached. The later slow adsorption rate is attributed to the electrostatic hindrance caused by already adsorbed vanadium species and the slow pore diffusion of the ions (Mekonnen et al., 2015). The results were interpreted using adsorption kinetic models that give insights into the possible rate-controlling steps and from which preliminary design parameters may be obtained. The kinetic models considered are pseudo-first-order (Equation 7), pseudo-second-order (Equation 8), and Elovich models (Equation 9).

$$\log\left(q_e - q_t\right) = \log q_e - \frac{k_1}{2.303}t \tag{8}$$

$$\frac{t}{q_t} = \frac{1}{k_2 q_e} + \frac{1}{q_e}t \tag{9}$$

$$q_t = \frac{1}{\beta}\ln\alpha\beta + \frac{1}{\beta}\ln t \tag{10}$$

where q_e and q_t are the adsorption capacity (mg/g) of solute at equilibrium and at a time t (min), respectively, k_1 (min^{-1}) and k_2 (g/mg·min) are the rate constants of the pseudo-first-order and pseudo-second-order adsorption, respectively. α is the initial adsorption rate (mg/g·min) and β is the desorption constant (g/mg) related to the extent of surface coverage and activation energy for chemisorption.

The kinetic model parameters and the linear regression values are presented in **Table 4**. The linear regression values obtained from the pseudo-second-order model are higher compared to the other two models, suggesting that the interaction between the adsorbent and V followed the pseudo-second-order mechanism and that this interaction was chemical in nature, further supporting the FTIR characterization results presented in earlier sections. Also revealed in **Table 4** is the increase

TABLE 3 | Comparison of capacity values between modified CNC and different waste-derived adsorbents in V removal.

Adsorbent	Sorption capacity q_m (mg/g)	References
Cassava waste biomass	20.0	Simate et al., 2015
Nano-sized banana peels	27.94	Oyewo et al., 2018
Brown seaweed (Biomass)	43.3	
Metal sludge	24.8	
Posidonia oceanica biomass	18.0	Pennesi et al., 2013
HDTMA-Br/CNC	47.2	Present study

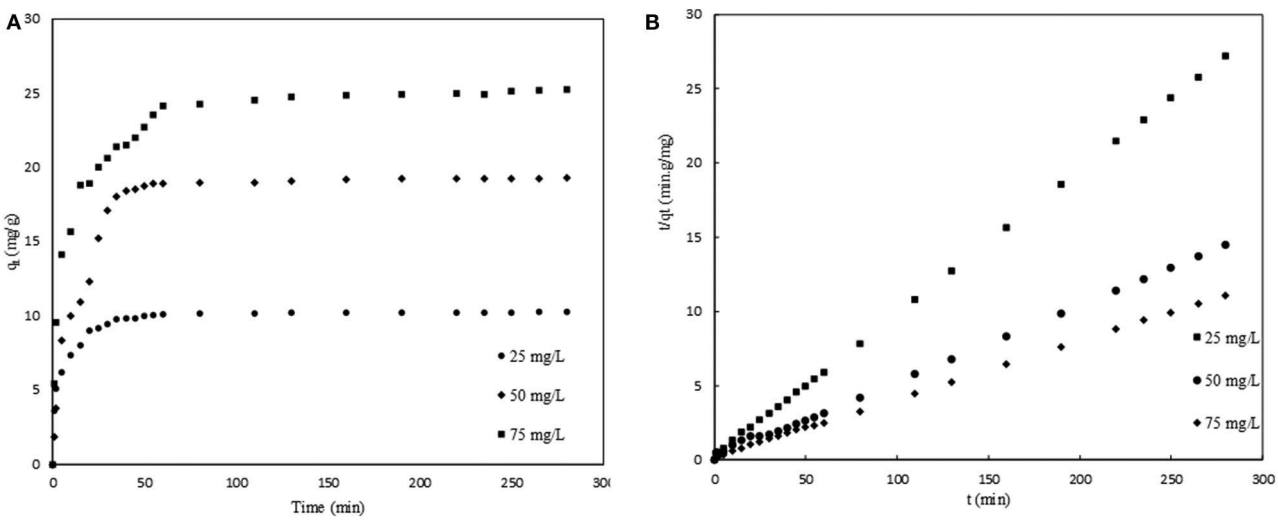

FIGURE 7 | (A) Adsorption kinetics for adsorption of V (V) onto modified CNC (HDTMA-Br/CNC) at different concentrations. **(B)** Pseudo-second-order kinetics model.

TABLE 4 | Kinetics parameters of V adsorption onto surfactant modified CNC.

Initial conc. (mg/L)		Pseudo-first order			Pseudo-second order			Elovich		
	q_e (mg g^{-1})	$q_{e,cal}$ (mg g^{-1})	k_1	R^2	$q_{e,cal}$ (mg g^{-1})	k_2	R^2	α	β	R^2
25	10.3	1.303	0.018	0.798	10.4	0.041	0.999	1.359	12.1	0.808
50	19.3	2.129	0.024	0.863	19.8	0.009	0.999	3.359	0.72	0.888
75	25.3	2.559	0.0.17	0.904	25.6	0.007	0.998	3.740	1.54	0.906

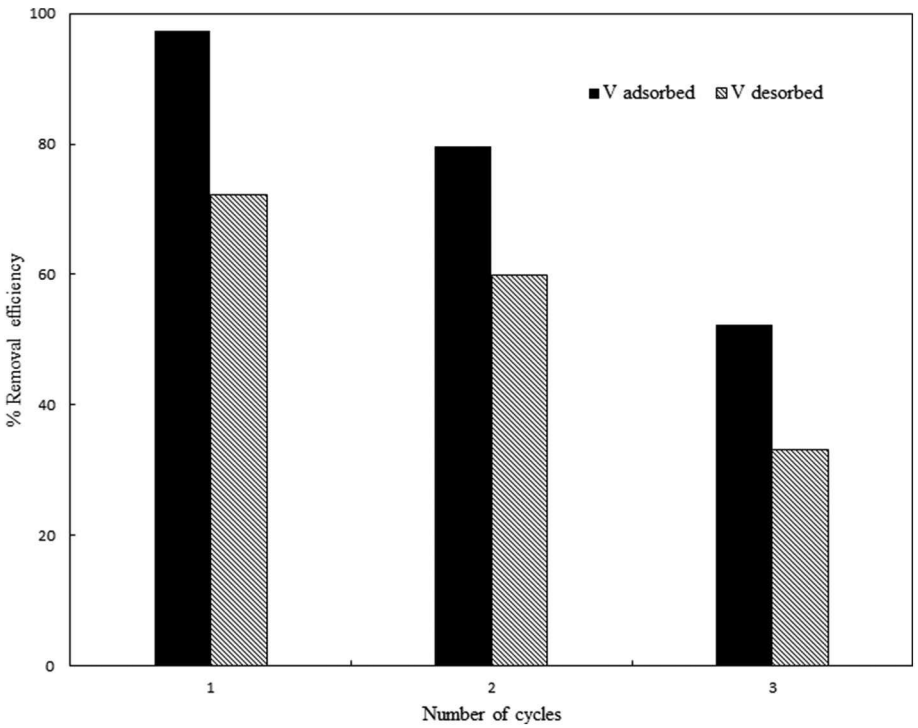

FIGURE 8 | Adsorption–desorption efficiency of vanadium using 2.0 M NaCl eluents.

in experimental adsorption capacity, q_e, with an increase in initial concentration. This is due to the higher driving force usually occurring at higher initial concentration of solute that overcomes the resistance of the mass transfer between bulk solution and the solid–liquid interface (Mthombeni et al., 2018). The experimental equilibrium capacities are very close to those determined using the pseudo-second-order model, which further point to the fact that indeed the process followed the pseudo-second-order mechanism.

Desorption Studies

The cyclic adsorption–desorption experiments were performed to evaluate the reusability of modified CNC to assess the economic viability of the adsorption process. Furthermore, reusability is also key to saving the environment from secondary pollution as a result of the disposal of the metal-loaded adsorbent. Three different eluents were investigated during the preliminary studies but only one (NaCl) was found to perform and was therefore chosen for subsequent desorption process. The adsorption–desorption results are presented in **Figure 8**. Two features are observed. First, both the adsorption and desorption efficiencies decrease in each operation cycle. For example, about 20% reduction in adsorption percentage was observed after the first cycle. Second, in each cycle, the adsorption efficiency is higher than that of desorption. Several reasons could explain the observations. The decrease in adsorption efficiency in each cycle is because not all active sites are released during the desorption step, rendering the adsorbent to lose its activity. Also, the decrease in desorption efficiency in each cycle is a manifestation of the strong bonds formed between the adsorbing vanadium ions and active sites. Moreover, the observations could also be ascribed to the dissolution of CNC and subsequent loss in mass of the adsorbent, which might have affected the mechanisms of interaction between V and the modified CNC active sites (Han et al., 2006). Overall, the adsorption–desorption results suggest that the modified-CNC could be reused more than once. Similar results were reported for the adsorption of cadmium and the reusability of brown seaweed derived cellulosic biosorbent using NaCl as an efficient eluent (Stirk and Staden, 2002).

CONCLUSION

CNC was successfully modified using HDTMA-Br, and its performance in V removal from water is explored. Characterization results of modified CNC showed dramatic improvement in the surface properties, which resulted in the enhancement of its adsorption capacity. The Langmuir adsorption isotherm model described the experimental data satisfactorily well-compared to other isotherm models. Meanwhile a rapid adsorption rate was observed as a result of availability of sufficient high-affinity binding sites at the initial stages of adsorption. In interpreting the kinetics of adsorbent–adsorbate interaction, a number of kinetic models were tested and results reveal that the pseudo-second-order model gives the best description of the data.

Indeed, therefore, the characterization and adsorption results point to the chemisorption nature of V interaction with modified CNC. In performing adsorption–desorption experiments to explore reusability of the adsorbent, it was observed that the media is reusable; however, the activity of the media decreased in each cycle. In general, the study demonstrated that modified CNC could be used as a promising adsorbent for removal of V from water. Further studies are ongoing to explore the applicability of this media in different water matrices.

DATA AVAILABILITY STATEMENT

All datasets generated for this study are included in the article/supplementary material.

AUTHOR CONTRIBUTIONS

All authors conceptualized the idea and experimental aspect. BZ and OO wrote the draft. BS and MO coordinated and corrected the final draft of the paper. TL coordinated and corrected the revised version of the manuscript.

ACKNOWLEDGMENTS

The authors would like to acknowledge the Tshwane University of Technology, Department of Science and Technology–Republic of South Africa for financial support of the Biorefineries Consortium and the Council for Scientific and Industrial Research (CSIR) for providing raw CNC and allowing access to analytical facilities.

REFERENCES

Abdullah, R., Abustan, I., and Ibrahim, A. N. M. (2013). Wastewater treatment using bentonite, the combinations of bentonite-zeolite, bentonite-alum, and bentonite-limestone as adsorbent and coagulant. *Int. J. Environ. Sci.* 4, 379–391. doi: 10.6088/ijes.2013040300014

Ahmad, M. A., Ahmad, N., and Bello, O. S. (2015). Removal of remazol brilliant blue reactive dye from aqueous solutions using watermelon rinds as adsorbent. *J. Dispersion Sci. Technol.* 36, 845–858. doi: 10.1080/01932691.2014.925400

Al-ghouti, M. A., and Da'ana, D. A. (2020). Guidelines for the use and interpretation of adsorption isotherm models: a review. *J. Hazard. Mater.* 393:122383. doi: 10.1016/j.jhazmat.2020.122383

Barakat, M. (2011). New trends in removing heavy metals from industrial wastewater. *Arabian J. chem.* 4, 361–377. doi: 10.1016/j.arabjc.2010.07.019

Bezerra, R. C., Leal, R. S., Da silva, M. I. S., Morais, A., Marques, T. A., Osajima, J. B., et al. (2017). Direct modification of microcrystalline cellulose with ethylenediamine for use as adsorbent for removal amitriptyline drug from environment. *Molecules* 22:E2039. doi: 10.3390/molecules22112039

Burakov, A. E., Galunin, E. V., Burakova, I. V., Kucherova, A. E., Agarwal, S., Tkachev, A. G., et al. (2018). Adsorption of heavy metals on conventional and nanostructured materials for wastewater treatment purposes: a review. *Ecotoxicol. Environ. Saf.* 148, 702–712. doi: 10.1016/j.ecoenv.2017.11.034

Carolin, F., Ponnusamy, S. K., Anbalangan, S., Joshiba, J., Naushad, M. (2017). Efficient Techniques for the Removal of Toxic Heavy Metals from Aquatic Environment: A Review. *J. Environ. Chem. Eng.* 5:3. doi: 10.1016/j.jece.2017.05.029

Gibril, M., Tesfaye, T., Sithole, B., Lekha, P. and Ramjugernath, D. (2018). Optimisation and enhancement of crystalline nanocellulose production by ultrasonic pretreatment of dissolving wood pulp fibres. *Cellulose Chem. Technol.* 52, 9–10. doi: 10.3390/molecules22112039

Han, R., Zhang, J., Zou, W., Shi, J., Xiao, H., and Liu, H. M. (2006). Biosorption of copper(II) and lead(II) from aqueous solution by chaff in a fixed bed column. *J. Hazard. Mater.* 133, 262–268. doi: 10.1016/j.jhazmat.2005.10.019

Hegazi, H. A. (2013). Removal of heavy metals from wastewater using agricultural and industrial wastes as adsorbents. *HBRC J.* 9, 276–282. doi: 10.1016/j.hbrcj.2013.08.004

Hokkanen, S., Bhatnagar, A., and Sillanpä, M. (2016). A review on modification methods to cellulose-based adsorbents to improve adsorption capacity. *Water Res.* 91,156–173. doi: 10.1016/j.watres.2016.01.008

Ince, M., and Ince, O. K. (2017). An Overview of adsorption technique for heavy metal removal from water/wastewater: a critical review. *Int. J. Pure Appl. Sci.* 3,10–19. doi: 10.29132/ijpas.358199

Jiang, Q., Xing, X., Jing, Y., and Han, Y. (2020). Preparation of cellulose nanocrystals based on waste paper via different systems. *Int. J. Biol. Macromol.* 149, 1318–1322. doi: 10.1016/j.ijbiomac.2020.02.110

Kaboorani, A., and Riedl, B. (2015). Surface modification of cellulose nanocrystals (CNC) by a cationic surfactant. *Ind. Crops Prod.* 65,45–55. doi: 10.1016/j.indcrop.2014.11.027

Kajjumba, G. W., Aydin, S., and Güneysu, S. (2018). Adsorption isotherms and kinetics of vanadium by shale and coal waste. *Adsorpt. Sci. Technol.* 36, 936–952. doi: 10.1177/0263617417733586

Kumar, R., Sharma, R. K., and Singh, A. P. (2017). Cellulose based grafted biosorbents - Journey from lignocellulose biomass to toxic metal ions sorption applications - a review. *J. Mol. Liq.* 232, 62–93. doi: 10.1016/j.molliq.2017.02.050

Li, J., Xiao, F., Zhang, L., and Amirkhanian, S. N. (2019). Life cycle assessment and life cycle cost analysis of recycled solid waste materials in highway pavement: A review. *J. Clean. Prod.* 233, 1182–1206. doi: 10.1016/j.jclepro.2019.06.061

Lizundia, E., Meaurio, E., and Vilas, J. (2016). "Grafting of cellulose nanocrystals," in *Multifunctional Polymeric Nanocomposites Based on Cellulosic Reinforcements*, eds P. Debora, E. Fortunati, J. M. Kenny (Elsevier), 61–113. doi: 10.1016/B978-0-323-44248-0.00003-1

Mahfoudhi, N., and Boufi, S. (2017). Nanocellulose: a challenging nanomaterial towards environment remediation. *Cell. Reinfor. Nanofibre Composites* 2017, 277–304. doi: 10.1016/B978-0-08-100957-4.00012-7

Mekonnen, E., Yitbarek, M., and Soreta, T. R. (2015). Kinetic and thermodynamic studies of the adsorption of Cr (VI) onto some selected local adsorbents. *South Afr. J. Chem.* 68, 45–52. doi: 10.17159/0379-4350/2015/v68a7

Mojiri, A., Hui, W., Arshad, A. K., Ridzuan, A. R. M., Hamid, N., Farraji, H., et al. (2017). Vanadium(V) removal from aqueous solutions using a new composite adsorbent (BAZLSC): Optimization by response surface methodology. *Adv. Environ. Res*, 6, 173–187. doi: 10.12989/aer.2017.6.3.173

Montaña, M., Camacho, A., Serrano, I., Devesa, R., Matia, L., and Vallés, I. (2013). Removal of radionuclides in drinking water by membrane treatment using ultrafiltration, reverse osmosis and electrodialysis reversal. *J. Environ. Radioact.* 125, 86–92. doi: 10.1016/j.jenvrad.2013.01.010

Mthombeni, N. H., Mbakop, S., Ochieng, A., and Onyango, M. S. (2016). Vanadium(V) adsorption isotherms and kinetics using polypyrrole coated magnetized natural zeolite. *J. Taiwan Inst. Chem. Eng.* 66, 172–180. doi: 10.1016/j.jtice.2016.06.016

Mthombeni, N. H., Mbakop, S., Ochieng, A., and Onyango, M. S. (2018). Adsorptive removal of V (V) ions using clinoptilolite modified with polypyrrole and iron oxide nanoparticles in column studies. *MRS Adv.* 3, 2119–2127. doi: 10.1557/adv.2018.229

Mulas, D., camacho, A., Serrano, I., Montes, S., Devesa, R., and Duch, M.A. (2017). Natural and artificial radionuclides in sludge, sand, granular activated carbon and reverse osmosis brine from a metropolitan drinking water treatment plant. *J. Environ. Radioact.* 177, 233–240. doi: 10.1016/j.jenvrad.2017.07.001

Nkalane, A., Oyewo, O. A., Leswifi, T., and Onyango, M. S.(2019). Application of coagulant obtained through charge reversal of sawdust-derived cellulose nanocrystals in the enhancement of water turbidity removal. *Mat. Res. Exp.* 6:105060. doi: 10.1088/2053-1591/ab3b49

Onyango, M. S., Kojima, Y., Aoyi, O., Bernardo, E. C., and Matsuda, H. (2004). Adsorption equilibrium modeling and solution chemistry dependence of fluoride removal from water by trivalent-cation-exchanged zeolite F-9. *J. Colloid Interf. Sci.* 279, 341–350. doi: 10.1016/j.jcis.2004.06.038

Oyewo, O. A., Wolkersdorfer, C., Onyango, M. S., and Adeniyi, A. (2018). "The performance of nano-sized Banana Peels in the removal of vanadium from mine water" in *11th ICARD | IMWA | MWD Conference – "Risk to Opportunity"*. South Africa.

Parmar, M., and Thakur, L. S. (2013). Heavy metal Cu, Ni and Zn: toxicity, health hazards and their removal techniques by low cost adsorbents: a short overview. *Int. J. Plant Anim. Environ. Sci.* 3, 2231–4490. Available online at: www.ijpaes.com.

Pennesi, C., Totti, C., and Beolchini, F. (2013). Removal of vanadium (III) and molybdenum (V) from wastewater using *Posidonia oceanica* (Tracheophyta) biomass. *PLoS ONE* 8:e76870. doi: 10.1371/journal.pone.0076870

Putro, J. N., Kurniawan, A., Ismadji, S., and Ju, Y.-H. (2017). Nanocellulose based biosorbents for wastewater treatment: study of isotherm, kinetic, thermodynamic and reusability. *Environ. Nanotechnol. Monit. Manage.* 8, 134–149. doi: 10.1016/j.enmm.2017.07.002

Quesada, H. B., Baptista, A. T. A., Cusioli, L. F., Seibert, D., De oliveira, B. C., and Bergamasco, R. (2019). Surface water pollution by pharmaceuticals and an alternative of removal by low-cost adsorbents: a review. *Chemosphere* 222, 766–780. doi: 10.1016/j.chemosphere.2019.02.009

Roy, S., Tang, M., and Edwards, M. A. (2019). Lead release to potable water during the Flint, Michigan water crisis as revealed by routine biosolids monitoring data. *Water Res.* 160, 475–483. doi: 10.1016/j.watres.2019.05.091

Salehi, S., and Anbia, M. (2019). Performance comparison of chitosan–clinoptilolite nanocomposites as adsorbents for vanadium in aqueous media. *Cellulose* 26, 1–25. doi: 10.1007/s10570-019-02450-9

Schwanningerab, M. (2004). Effects of short-time vibratory ball milling on the shape of FT-IR spectra of wood and cellulose. *Vibrat. Spectrosc.* 36, 23–40. doi: 10.1016/j.vibspec.2004.02.003

Simate, G. S., Ndlovu, S., and Seepe, L. (2015). Removal of heavy metals using cassava peels waste biomass in a multi-stage countercurrent batch operation. *J. S. Afr. Inst. Min. Metall.* 115, 1137–1141. doi: 10.17159/2411-9717/2015/v115n12a1

Singh, K., Sinha, T. J. M., and Srivastava, S. (2015). Functionalized nanocrystalline cellulose: smart biosorbent for decontamination of arsenic. *Int. J. Mineral Process.* 139, 51–63. doi: 10.1016/j.minpro.2015.04.014

Sithole, B. (2019). *Beneficiation of Pulp and Paper Mill Sludge*. Clean Technologies and Environmental Policy. doi: 10.1016/B978-0-323-44248-0.00003-1

Stirk, W., and Staden, V. (2002). desorption of cadmium and the reuse of brown seaweed derived products as biosorbents. *Bot. Marina* 45, 9–16. doi: 10.1515/BOT.2002.002

Yin, X., Meng, X., Zhang, Y., Zhang, W., Sun, H., Lessl, J. T., et al. (2018). Removal of V (V) and Pb (II) by nanosized TiO2 and ZnO from aqueous solution. *Ecotoxicol. Environ. Saf.* 164, 510–519. doi: 10.1016/j.ecoenv.2018.08.066

Conflict of Interest: The authors declare that the research was conducted in the absence of any commercial or financial relationships that could be construed as a potential conflict of interest.